Beyond Flory-Huggins Theory: New Classes of Blend Miscibility Associated with Monomer Structural Asymmetry

Jacek Dudowicz,[1] Karl F. Freed,[1] and Jack F. Douglas[2]

[1]*The James Franck Institute, The University of Chicago, Chicago, Illinois 60637*

[2]*Polymers Division, Institute of Standards and Technology, Gaithersburg, Maryland 20899*

(Received 12 November 2001; published 13 February 2002)

Flory-Huggins (FH) theory is restricted to polymer mixtures whose monomers are structurally identical, a situation limited to isotopic blends and computer simulations. We investigate the influence of monomer structure on blend miscibility and scattering properties using the lattice cluster theory generalization of the FH model. Monomer structural asymmetry is shown to profoundly affect blend miscibility (T_c, ϕ_c), chain swelling (T_θ), and the scale (ξ) and intensity $[S(0)]$ of composition fluctuations. Four distinct blend miscibility classes are identified and experimental evidence for these classes is discussed.

DOI: 10.1103/PhysRevLett.88.095503 PACS numbers: 61.25.Hq, 05.50.+q, 05.70.Jk, 64.60.Fr

Many commercially important materials are "alloys" of polymers having different chemical and physical characteristics, and the stability and state of dispersion of polymer blends are often crucial in applications. Flory-Huggins (FH) theory [1] has long provided a basis for understanding the thermodynamic properties of these mixtures, and the theory is also an essential input into the analysis of blend scattering [2] and into kinetic models of blend phase separation [3]. More generally, FH theory is widely used in treatments of systems containing biological polymers [4]. While FH theory explains some basic trends in blend miscibility (e.g., limited miscibility of high molecular mass blends), the theory *completely neglects* the dissimilarity in monomer structure that is central to the fabrication of real blends. A number of approaches (integral equation theory [5], Monte Carlo simulations [6], continuum field theory [7], and analytic lattice model calculations [8]) give insights into the physics of polymer blends, but no theory has emerged that can predict analytically how monomer structure affects blend miscibility.

We systematically investigate the influence of monomer structure on blend miscibility using the lattice cluster theory (LCT) [8] generalization of the FH model. Analytic calculations are rendered tractable by restricting the analysis to the limit of incompressible, high molecular weight blends [9]. The well-known miscibility pattern predicted by FH theory is recovered *only* for a limited range of monomer size and shape asymmetries, but when the monomers have dissimilar structures, the LCT yields *three additional* blend miscibility classes whose behaviors are quite different from the predictions of classical FH theory.

The LCT [8,9] is based on two major improvements beyond the leading order FH approximation to the blend free energy. First, united atom models are used to represent individual monomers as occupying several neighboring lattice sites, as illustrated in Fig. 1 for a few polyolefins considered in this paper. The second improvement involves a superior solution to the resulting lattice model. Corrections to the FH free energy (from nonrandom mixing) are systematically derived in the form of a high temperature, $1/d$ cluster expansion [8]. The LCT is rendered analytically tractable by confining attention to the high pressure, high molecular weight, and fully flexible chain limit, termed the simplified LCT (SLCT).

The SLCT free energy of mixing $\Delta f^{\rm mix}$ for a binary homopolymer blend equals [9]

$$\frac{\Delta f^{\rm mix}}{kT} = \frac{\phi}{M}\ln\phi + \frac{1-\phi}{M\lambda}\ln(1-\phi) + \phi(1-\phi)\left[\frac{(r_1-r_2)^2}{z^2} + \frac{\epsilon}{kT}\left(\frac{z-2}{2} - \frac{1}{z}\{p_1(1-\phi) + p_2\phi\}\right)\right], \quad (1)$$

where $\phi \equiv \phi_1 = 1 - \phi_2$ is the volume fraction of component 1, $M \equiv M_1$ is the number of united atom groups in a single chain of blend species 1, $\lambda = M_2/M_1$, $\epsilon = \epsilon_{11} + \epsilon_{22} - 2\epsilon_{12}$ is the blend exchange energy, z is the lattice coordination number, and T is the absolute temperature. The chain occupancy index $M_i = N_i s_i$ (where s_i denotes the number of lattice sites occupied by a single monomer) reduces to the polymerization index N_i only when $s_i = 1$. The first two terms on the right-hand side of Eq. (1) represent the configurational entropy, while $[\phi(1-\phi) \times (r_1 - r_2)^2/z^2]$ is the noncombinatorial entropy of mixing which arises from packing constraints imposed by the monomer structures. The entropic coefficients r_i $(i = 1, 2)$ are obtained from the respective numbers $s_i^{(3)}$ and $s_i^{(4)}$ of tri- and tetrafunctional united atom groups in a single monomer of species i as $r_i = 1 + s_i^{(3)}/s_i + 3s_i^{(4)}/s_i$. The remaining energetic terms in Eq. (1) involve both monomer structure dependent and independent contributions. The monomer structure dependence enters through the geometrical factors p_1 and p_2, which equal the numbers of distinct sets of three sequential bonds traversing single monomers of species 1 and 2, respectively. Reference [9] tabulates r_i and p_i for a wide range of

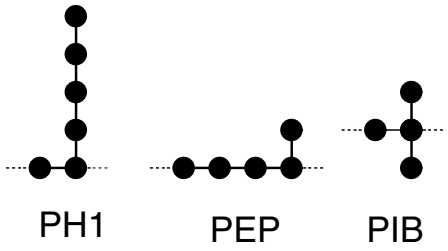

FIG. 1. United atom group models for monomers of poly(hexene-1) (PH1), poly(ethylene propylene) (PEP), and poly(isobutylene) (PIB). Circles designate CH_n groups, solid lines represent the C-C bonds inside the monomer, and dotted lines indicate the C-C bonds that link the monomer's CH_n groups with the polyolefin chain backbone. The branching parameters r_i and p_i equal $r_{\mathrm{PH1}} = 7/6$, $p_{\mathrm{PH1}} = 4/3$, $r_{\mathrm{PEP}} = p_{\mathrm{PEP}} = 6/5$, $r_{\mathrm{PIB}} = 7/4$, and $p_{\mathrm{PIB}} = 3/2$.

monomer structures and discusses their evaluation. The leading energetic contribution of $z\epsilon/(2kT)$ is merely the FH interaction term which grossly overestimates the number of nearest neighbor heterocontacts. The replacement of the factor of z in the FH approximation $z\epsilon/(2kT)$ by $(z - 2)$ represents a first correction to this contact number [10].

The small angle neutron scattering χ parameter in the incompressible limit is defined in terms of the free energy Δf^{mix},

$$\left.\frac{\partial^2(\Delta f^{\mathrm{mix}}/kT)}{\partial\phi^2}\right|_{T,V} = \frac{1}{M\phi} + \frac{1}{M\lambda(1-\phi)} - 2\chi\,, \tag{2}$$

where χ is expressed as an interaction parameter between united atom groups [9,11]. Evaluating the derivative in Eq. (2) converts χ into the simple polynomial $\chi = a + (b + c\phi)/T$, where

$$\begin{aligned} a &= (r_1 - r_2)^2/z^2, \\ b &= (\epsilon/k)[(z-2)/2 + (1/z)(-2p_1 + p_2)], \\ c &= (\epsilon/k)(3/z)(p_1 - p_2)\,. \end{aligned} \tag{3}$$

The sign of b determines the type of phase separation [upper critical solution temperature (UCST) versus lower critical solution temperature (LCST) phase diagram]. When both blend components have monomers with the same structures, a and c *vanish*.

The critical composition ϕ_c is determined by the condition, $\partial^3\Delta f^{\mathrm{mix}}/\partial\phi^3|_{\phi=\phi_c} = 0$, which, in combination with Eq. (1), yields

$$-2ac\phi_c^2(1-\phi_c)^2 + [2c(\lambda-1)\phi_c^3 + \{b(\lambda-1) - c(4\lambda-1)\}\phi_c^2 + 2(c-b)\lambda\phi_c + b\lambda]/(M\lambda) = 0\,. \tag{4}$$

The critical temperature T_c is evaluated from the stability condition obtained by setting Eq. (2) to zero and inserting the expression for ϕ_c from Eq. (4) into the resulting equation,

$$T_c = \frac{2(b + c\phi_c)}{1/(M\phi_c) + 1/[M\lambda(1-\phi_c)] - 2a}\,. \tag{5}$$

The largest contribution to the shift of T_c from its FH value is due to the parameter a. An increase of a generally leads to decreased blend miscibility.

The correlation length amplitude ξ_o [$\xi \equiv \xi_o(|T - T_c|/T)^{-1/2}$] is another characteristic property of polymer blends that is strongly influenced by monomer shape and size asymmetries (our results are derived in mean field theory, which is valid [2,12] sufficiently far from T_c). Within the SLCT, ξ_o is expressed as

$$\xi_o = [d_o T_c/(2|b + c\phi_c|)]^{1/2}. \tag{6}$$

d_o is the square gradient coefficient, determined from random phase approximation (RPA) [2], and ξ_o is thus *independent* of T. The mean field sum rule $\xi^2 \sim S(0)$ [ξ is the static correlation length and $S(0)$ is the structure factor in the long wavelength limit] implies that ξ_o controls both the amplitude [$S(0)$] and the scale (ξ) of composition fluctuations [13].

In analogy to polymer solutions, where the theta temperature T_θ is normally identified as an essential reference temperature [1,2], T_θ can also be defined (and measured) for dilute polymer blends. Since either component of a binary blend can be the dilute species, there are *two* osmotic virial expansions and *two* theta temperatures. Within the SLCT, the $T_\theta^{(1)}$ and $T_\theta^{(2)}$ are evaluated as

$$T_\theta^{(1)} = \frac{2(b + c)M_1}{1 - 2aM_1}\,, \qquad T_\theta^{(2)} = \frac{2bM_2}{1 - 2aM_2}\,. \tag{7}$$

For $\lambda = 1$, $T_\theta^{(1)} \approx T_\theta^{(2)} \equiv T_\theta$, and $\delta T_\theta^{(1)} \approx \delta T_\theta^{(2)}$, where $\delta T_\theta^{(i)} \equiv (T_\theta^{(i)} - T_c)/T_c$, since $|c/b|$ is normally small [9], so in this case we suppress the superscript (i). The $T_\theta^{(i)}$ have the same significance for chain swelling as they do in polymer solutions [14].

The SLCT predicts that binary polymer blends yield four distinct classes of critical behavior. This classification is based on the analysis of Eqs. (3)–(7) which enable the evaluation of the critical parameters $(\phi_c, T_c, \xi_o, T_\theta^{(1)}, T_\theta^{(2)})$ for eight potential types of blends that arise because b may be either sign and because a and c may be either zero or nonzero. a is positive in the SLCT, while b and c can be of either sign. (The classes of critical behavior for $a < 0$ are not detailed here as they do not emerge from the SLCT for polymer blends.)

In addition to different monomer structures, the blend components usually have different M_i. This introduces an additional source of asymmetry (particle exchange symmetry) quantified in the LCT by the chain occupancy index ratio $\lambda = (M_2/M_1)$, an extension of the polymerization index ratio $\lambda_N = (N_2/N_1)$ in FH theory to account for differences in monomer sizes. We next summarize some of

the essential characteristics of the four classes of blends indicated by the SLCT.

Class I [$a = 0, b > 0, c = 0$ (or $c \neq 0$)] (similar to FH theory) is characterized by a UCST phase separation in which T_c is proportional to M and ϕ_c depends only on λ. Class I:

$$\phi_c \cong \phi_c^{(I)} \equiv \sqrt{\lambda}/(1 + \sqrt{\lambda}), \qquad T_c \sim M, \qquad \xi_o \sim M^{1/2}, \qquad \delta T_\theta^{(1)}, \delta T_\theta^{(2)} = g_i(\lambda),$$

where $g_i(\lambda = 1) = 3$. $\phi_c^{(I)}$ represents the correction of $\phi_c^{(\mathrm{FH})} = \sqrt{\lambda_N}/(1 + \sqrt{\lambda_N})$ for differences in monomer volumes [1]. The remaining three classes exhibit *qualitative departures* from FH behavior. Class II [$a \neq 0, b > 0, c = 0$ (or $c \neq 0$)] also yields a UCST behavior, but with a *nonlinear* dependence of T_c on M. On the other hand, ϕ_c remains identical to $\phi_c^{(\mathrm{I})}$ for the FH class I. Class II:

$$\phi_c \cong \phi_c^{(\mathrm{I})}, \qquad T_c \sim \frac{M}{1 - 2alM}, \qquad \xi_o \sim \frac{M^{1/2}}{(1 - 2alM)^{1/2}}, \qquad \delta T_\theta^{(1)}, \delta T_\theta^{(2)} \sim \frac{1}{1 - 2a\lambda M},$$

where $l \equiv \lambda/(1 + \sqrt{\lambda})^2$. The occurrence of a UCST phase diagram is limited, however, to values of M below $M_c = 1/(2al)$ where T_c *diverges*.

Class III ($a \neq 0, b < 0, c = 0$) is our first example producing LCST behavior and dramatic departures from the FH pattern of blend miscibility. T_c in the $M \to \infty$ limit no longer scales with M, but instead approaches a *constant* ($|b|/a$) as $M \to \infty$. ϕ_c remains equal to $\phi_c^{(\mathrm{I})}$ since $c = 0$. Class III:

$$\phi_c = \phi_c^{(\mathrm{I})}, \qquad T_c = |b|/a, \qquad \xi_o = \text{const}, \qquad \delta T_\theta^{(1)}, \delta T_\theta^{(2)} \sim M^{-1}.$$

Class IV ($a \neq 0, b < 0, c \neq 0$) also yields LCST phase separation, but there are important differences from class III. ϕ_c depends strongly on M and T_c approaches a constant in the $M \to \infty$ limit whose value depends on the sign of c. Class IV:

$$\phi_c \sim M^{-1/2}, \quad T_c = |b|/a, \quad \xi_o \sim M^{1/4}, \quad \delta T_\theta^{(1)} = c/b, \quad \delta T_\theta^{(2)} \sim M^{-1/2}, \quad (c < 0),$$
$$\phi_c = 1 - O(M^{-1/2}), \quad T_c = |b - c|/a, \quad \xi_o \sim M^{1/4}, \quad \delta T_\theta^{(1)} \sim M^{-1/2}, \quad \delta T_\theta^{(2)} = c/|b - c|, \quad (c > 0).$$

The remaining four of the eight possible blend types are either completely miscible or immiscible.

Figures 2(a)–2(d) graphically illustrate the dependence of these properties for some "symmetric" polyolefin blends ($\lambda = 1; M_1 = M_2 = M$) specified in the caption. The differences in the predicted dependence of T_c on M are shown in Fig. 2(a). The linear scaling of T_c with M corresponds to FH theory (class I); class II exhibits a stronger than linear M dependence of T_c; while T_c for classes III and IV approach constants. The critical composition [see Fig. 2(b)] is insensitive to M in classes I–III, but depends on M for class IV, decreasing towards zero (or unity) with the scaling $\phi_c \sim M^{-1/2}$. (Clearly, the FH estimate for ϕ_c can be grossly in error for LCST blends.) The correlation length amplitude ξ_o [see Fig. 2(c)] for class II increases with M more rapidly than for class I ($\xi_o \sim M^{1/2}$), but ξ_o for classes III and IV is significantly *smaller* than the chain radius of gyration ($R_g \sim M^{1/2}$). An insensitivity of ξ_o to M occurs in class III, where ξ_o is on the order of the statistical segment length rather than R_g. The deviation δT_θ of T_θ from T_c is also an indicator of the blend miscibility class. The large values of δT_θ for classes I and II suggest that T_θ is experimentally inaccessible. (Most polymers with T_c near room temperature would be thermally unstable at these T_θ.) In contrast, T_θ is predicted to be close to T_c for classes III and IV blends [14].

A linear scaling of T_c with M has been confirmed by small-angle neutron scattering (SANS) experiments [15] for symmetric ($N_1 = N_2$) isotopic polyolefin blends (where molecular monomer structures are almost identical) and by Monte Carlo simulations [6]. However, several experimental observations indicate that this FH pattern of blend miscibility is not general. Perhaps the best documented example of this nonuniversality is provided by the polystyrene/poly(vinyl methyl ether) (PS/PVME) blend. SANS experiments by Han and co-workers [16] reveal that T_c for this system is nearly insensitive to M ($T_c = 145 \pm 5$ °C), while ϕ_c is highly asymmetric even for samples with identical N_1 and N_2. Based on the constraints $b < 0$ and $a, c \neq 0$ (determined from our fits to the scattering data [8]), PS/PVME blends are classified as type IV blends. The SLCT prediction that $T_c \to (|b|/a)$ for class IV blends in the $M \to \infty$ limit accords with the constancy of T_c found by Han *et al.* [16]. Moreover, the SLCT scaling $\phi_c \sim M^{-1/2}$ is consistent with the additional finding [16] that a factor of 3 increase in M leads to a reduction of ϕ_c by roughly a factor of 2. Other measurements [16,17] for PS/PVME mixtures verify our predictions of a weak M-dependence of the correlation length amplitude ($\xi_o \sim M^{1/4}$) [see Fig. 2(c)] and the proximity between T_θ and T_c [see Fig. 2(d)]. All the predicted characteristics of class IV blends are thus verified.

A similar insensitivity of T_c to M has been observed [18] for binary blends of PIB with several other polyolefins, where it is difficult to imagine that any "specific interactions" could be responsible for the observed dramatic deviations from FH theory. (Notably, our explanation of the non-FH critical behavior for PS/PVME blends likewise does not require invoking "special" interactions.) The LCST phase separation in these systems is predicted

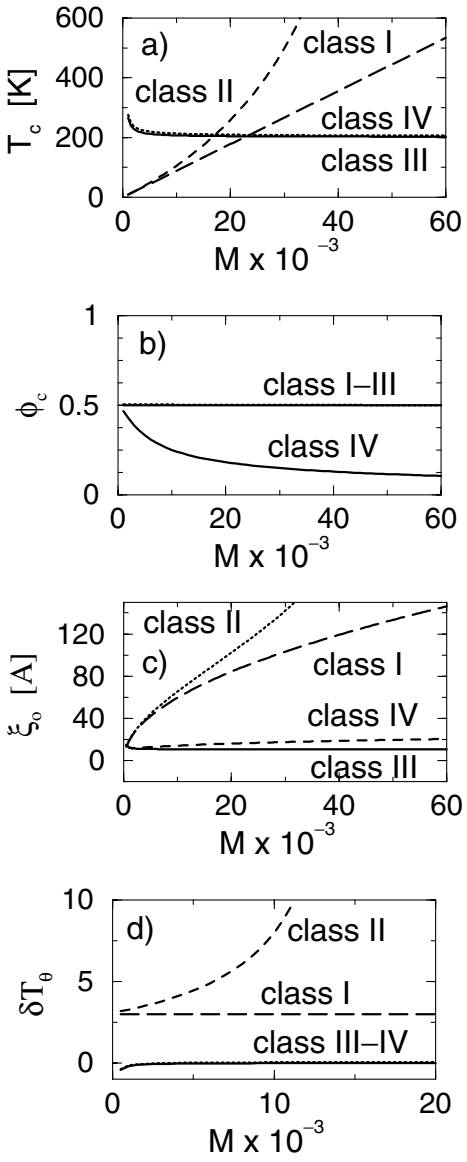

FIG. 2. The critical temperature T_c, critical composition ϕ_c, correlation length amplitude ξ_o, and reduced theta temperature $\delta T_\theta \equiv (T_\theta - T_c)/T_c$ for "symmetric" blends ($\lambda = 1; M_1 = M_2 = M$) as a function of the number of united atom groups M. (a) T_c; (b) ϕ_c; (c) ξ_o; (d) δT_θ. Classes II and IV are represented by PH1/PEP and PIB/PEP blends, respectively. The example for class I blends($a = c = 0, b > 0$) is derived by choosing b as identical to b for class II, while the example for class III blends ($a \neq 0, b < 0, c = 0$) is generated by taking a and b equal to those for the PIB/PEP system. The exchange energies ϵ for the PH1/PEP and PIB/PEP blends are taken as $\epsilon/k = 0.01$ K and $\epsilon/k = -1$ K, respectively [9].

to arise within the SLCT from the competition between a negative energetic portion of the χ parameter and a sufficiently positive "entropic" part a of χ. The PIB blends exhibit a large a part of the parameter χ due to the presence of a tetrafunctional carbon atom in the PIB monomer. The negative exchange energy ϵ (implying $b < 0$) may occur because 50% of the PIB united atom units are CH_3 groups that have larger attractive interactions (i.e., Lennard-Jones interaction parameters) than the CH_2, CH, and C united atom groups [19]. This effect produces a large self-interaction $\epsilon_{11} \equiv \epsilon_{\mathrm{PIB-PIB}}$ and a large heterocontact interaction ϵ_{12}, leading to a negative $\epsilon = \epsilon_{11} + \epsilon_{22} - 2\epsilon_{12}$.

Finally, we note that caution should be exercised in using the FH expression $\phi_c^{(\mathrm{FH})} = \sqrt{\lambda_N}/(1 + \sqrt{\lambda_N})$ to estimate T_c, ξ_o, and other critical properties of polymer blends since this can lead to substantial errors. It is necessary to determine ϕ_c from the measured coexistence curve.

This research is supported, in part, by NIH Grant No. GM56678. We thank M. Muthukumar and Frank Bates for stimulating discussions.

[1] P. J. Flory, *Principles of Polymer Chemistry* (Cornell University Press, Ithaca, NY, 1953).
[2] P. G. de Gennes, *Scaling Concepts in Polymer Physics* (Cornell University, Ithaca, NY, 1979).
[3] S. C. Glotzer, Annu. Rev. Comput. Phys. **2**, 1 (1995).
[4] P. S. Niranjan *et al.,* J. Chem. Phys. **114**, 10 573 (2001); G. B. Fields *et al.,* J. Chem. Phys. **96**, 3974 (1992); J. Herzfeld, Acc. Chem. Res. **29**, 31 (1996); X.-H. Guo and S.-H. Chen, Phys. Rev. Lett. **64**, 1979 (1990).
[5] K. S. Schweizer and J. G. Curro, Adv. Chem. Phys. **98**, 1 (1997).
[6] A. Sariban and K. Binder, J. Chem. Phys. **86**, 5859 (1987); Macromolecules **21**, 711 (1988); M. Müller and K. Binder, Macromolecules **28**, 1825 (1995); J. D. Weinhold *et al.,* J. Chem. Phys. **103**, 9460 (1995); F. A. Escobedo and J. J. de Pablo, Macromolecules **32**, 900 (1999).
[7] G. H. Fredrickson, A. J. Liu, and F. S. Bates, Macromolecules **27**, 2503 (1994).
[8] J. Dudowicz and K. F. Freed, Macromolecules **24**, 5076 (1991); **24**, 5112 (1991).
[9] K. F. Freed and J. Dudowicz, Macromolecules **31**, 6681 (1998).
[10] E. A. Guggenheim, Proc. R. Soc. London A **183**, 213 (1944); **183**, 303 (1944).
[11] J. Dudowicz and K. F. Freed, Macromolecules **33**, 9777 (2000).
[12] P. G. de Gennes, J. Phys. Lett. **38**, L441 (1977); K. Binder, J. Chem. Phys. **79**, 6387 (1983).
[13] J. Dudowicz *et al.,* J. Chem. Phys. **99**, 4804 (1993).
[14] R. M. Briber, B. J. Bauer, and B. Hammouda, J. Chem. Phys. **101**, 2592 (1994).
[15] M. D. Gehlsen *et al.,* Phys. Rev. Lett. **68**, 2452 (1992).
[16] C. C. Han *et al.,* Polymer **29**, 2002 (1988).
[17] Y. B. Melnichenko, G. D. Wignall, and D. Schwahn (unpublished).
[18] R. Krishnamoorti *et al.,* Macromolecules **28**, 1252 (1995).
[19] M. Mondello *et al.,* J. Chem. Phys. **105**, 5208 (1996).